Separation Science and Technology
Publication details, including instructions for authors and subscription information:
http://www.informaworld.com/smpp/title~content=t713708471

Liquid Membrane Separations of Metal Cations Using Macrocyclic Carriers

J. J. Christensen[a]; J. D. Lamb[a]; P. R. Brown[a]; J. L. Oscarson[a]; R. M. Izatt[a]
[a] DEPARTMENTS OF CHEMICAL ENGINEERING AND CHEMISTRY AND CONTRIBUTION, 251 FROM THE THERMOCHEMICAL INSTITUTE, BRIGHAM YOUNG UNIVERSITY, PROVO, UT

To cite this Article Christensen, J. J. , Lamb, J. D. , Brown, P. R. , Oscarson, J. L. and Izatt, R. M.(1981) 'Liquid Membrane Separations of Metal Cations Using Macrocyclic Carriers', Separation Science and Technology, 16: 9, 1193 — 1215
To link to this Article: DOI: 10.1080/01496398108057607
URL: http://dx.doi.org/10.1080/01496398108057607

SEPARATION SCIENCE AND TECHNOLOGY, 16(9), pp. 1193-1215, 1981

Liquid Membrane Separations of Metal Cations Using Macrocyclic Carriers

J. J. CHRISTENSEN*, J. D. LAMB*, P. R. BROWN, J. L. OSCARSON, and R. M. IZATT*

DEPARTMENTS OF CHEMICAL ENGINEERING AND CHEMISTRY AND CONTRIBUTION 251 FROM THE THERMOCHEMICAL INSTITUTE, BRIGHAM YOUNG UNIVERSITY, PROVO, UT 84602

ABSTRACT

The selectivity in water and methanol solvents of macrocyclic crown ether ligands toward univalent and bivalent cations is well known. Incorporation of these ligands into chloroform liquid membranes separating water and salt solution phases results in a system showing selective cation transport. The cation transport rates of single cations across these liquid membranes have been correlated with equilibrium constant values for cation-macrocycle interaction in methanol. This correlation has been extended to binary cation mixtures of Cs^+ with Li^+, Na^+, K^+, and Rb^+. A model for cation transport from these cation mixtures has been reduced to an equation which gives good agreement between measured and predicted transport rates across our liquid membranes.

INTRODUCTION

It has been nearly two decades since macrocycles of the polyether type were synthesized (1-3). Since that time there has been great interest in compounds of this type because they selectively complex cations and greatly enhance the solubilities of

salts in organic solvents, thereby making ions such as MnO_4^-, O_2^-, SCN^-, F^-, etc. available for chemical reaction in these solvents. The increased solubility in organic solvents of inorganic salts caused by macrocycles is impressive. For example, Pedersen (3) points out that when powdered $KMnO_4$ crystals are sprinkled on the surface of benzene the crystals settle to the bottom leaving no sign of their passage though the colorless liquid. However, repeating this process with a benzene solution containing dicyclohexano-18-crown-6 (see Fig. 1) results in the crystals leaving a trail of flashing purple. A solution exceeding 0.02 M $KMnO_4$ in benzene can be obtained in this manner.

The ability of macrocycles to solubilize cation salts in hydrophobic solvents makes them excellent candidates as cation carriers in membranes. Both the cation selectivity and the cation transport across the boundary between an aqueous and an organic phase by macrocycles of the type shown in Fig. 1 can be understood by reference to the type of complex formed between a cation and a macrocycle. The K^+-18-crown-6 complex is illustrated in Fig. 2. The K^+ is seen to be the correct size to lie within the symmetrical cavity formed by the 18-crown-6. Coordination to the inward-oriented oxygen donor atoms holds the K^+ in the center of the macrocycle cavity (4). The hydrophobic exterior of the macrocycle combined with the ease of ion-pair formation between the large positively charged complex and the accompanying anion make passage into an organic solvent feasible.

Of particular interest to those involved in cation separations are the properties of specificity (a) in the complexation of similar cations, and hence differentiation among these cations, and (b) in the carrier-mediated selective transport of cations across phase boundaries. Equilibrium constants, K, defined for reaction (1) by equation (2) have been determined in water, $K(H_2O)$,

$$M^{n+} + L = ML^{n+} \tag{1}$$

$$K = \frac{[ML^{n+}]}{[M^{n+}][L]} \tag{2}$$

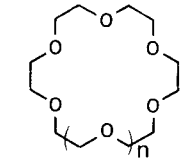

n = 0: 15-Crown-5 (15C5)
n = 1: 18-Crown-6 (18C6)
n = 2: 21-Crown-7 (21C7)

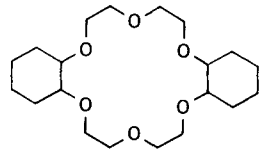

Dicyclohexano-18-Crown-6
(DCy18C6)

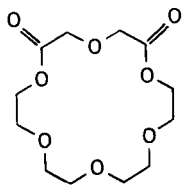

2,6-Diketo-18-Crown-6
(DK18C6)

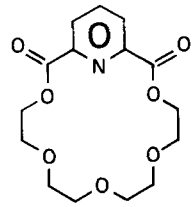

2,6-Diketo-4-Pyridyl-18-Crown-6
(DKP 18C6)

FIGURE 1. Representative macrocycles. Application of conventional IUPAC rules for naming organic compounds results in the assignment of unequivocal, but quite complicated names to the synthetic macrocyclic compounds of the cyclic polyether type. In the simplified nomenclature scheme used in this paper, the name of a cyclic polyether is derived in this order: the side ring substituents or replacement donor atoms (if any), the total number of atoms in the polyether ring, the word "crown" and the total number of donor atoms in the polyether ring. For example, the name 18-crown-6 is derived from the presence in the ring structure of eighteen total ring atoms (carbon and oxygen) and six donor oxygen atoms. The name dicyclohexano-18-crown-6 indicates the presence of two cyclohexo groups.

and methanol, $K(CH_3OH)$, solvents for the reaction of a large number of macrocyclic ligands (L) with alkali metal ions, alkaline earth metal ions, Ag^+, Tl^+, and Pb^{2+} (5). In addition, carrier-mediated cation transport across a chloroform liquid membrane has been studied for a variety of metal-macrocycle combinations (6), and a mathematical relationship has been developed which correctly

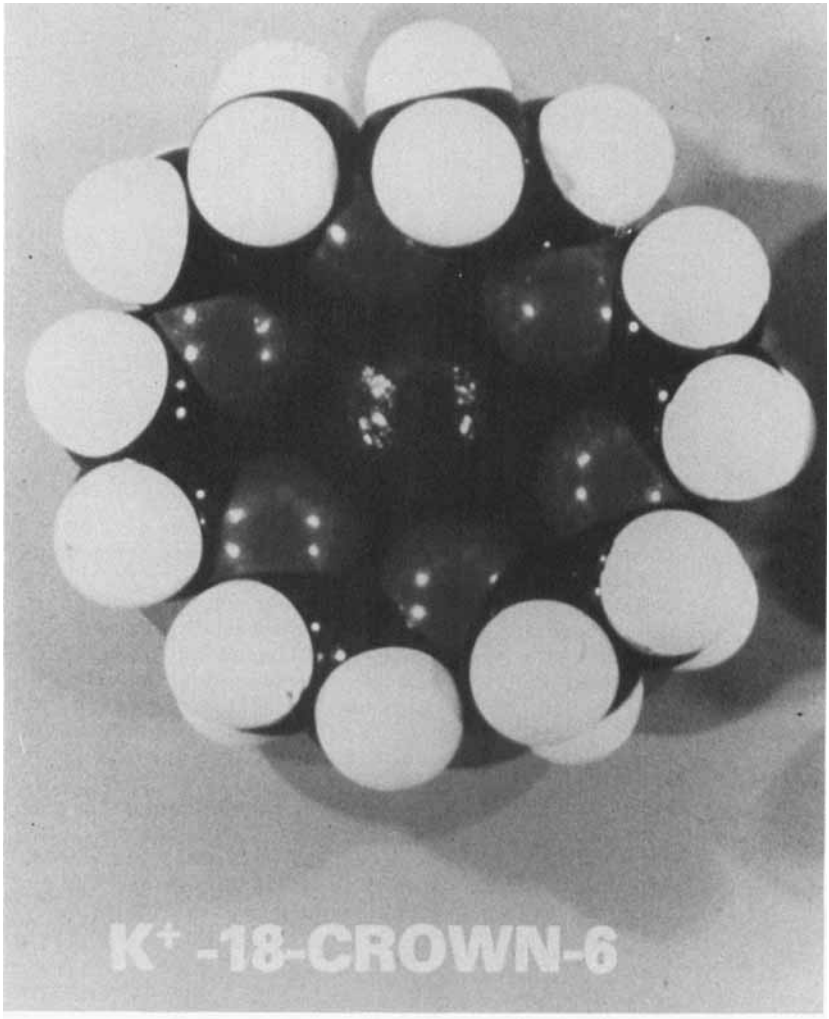

FIGURE 2. Representation of the K^+-18-crown-6 complex using CPK molecular models.

predicts cation transport rates for known values of log $K(CH_3OH)$ (7).

The purpose of this paper is to summarize results which have been obtained by us in the areas of cation complexation in methanol, cation transport across liquid membranes, and correlation of cation transport rates, J_M, with log $K(CH_3OH)$ both for unitary and binary cation systems.

EXPERIMENTAL

Materials

The salts used were the highest quality available. The macrocycles either were synthesized by J. S. Bradshaw and his coworkers at Brigham Young University or were obtained from Parish Chemical Company. Wherever possible, the purities of the macrocycles were determined by calorimetric titration to an endpoint against a standard cation solution (8).

Procedure

The log K (CH_3OH) values were determined by a calorimetric titration procedure which has been described (9). The use of this method to determine log K values can be understood by reference to Fig. 3 where a series of curves is depicted for the calorimetric titration of component B into component A. These curves are calculated for the reaction A + B = AB, by holding ΔH constant and allowing K to vary from infinity to ten. The shape of each curve is a function of both ΔH and K. However, as K increases the endpoint becomes sharper and the curvature decreases making calculation of K less precise. In practice, log K values between approximately 1 and 5 can be determined using the calorimetric

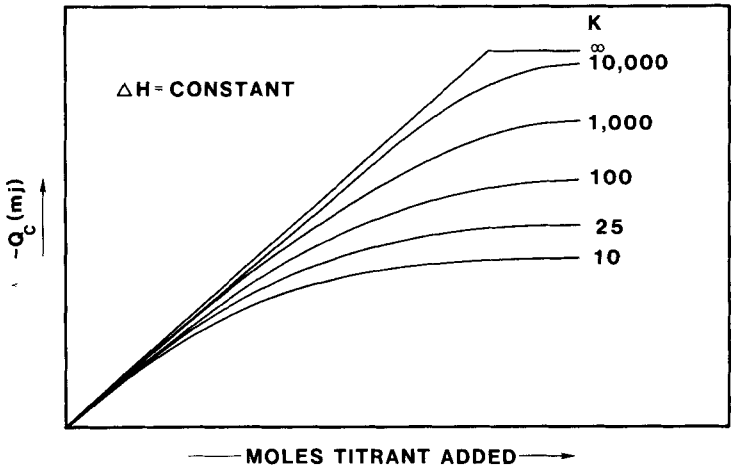

FIGURE 3. Plot of heat generated ($-Q_c$) during calorimetric titrations of A with B to produce AB (1:1 reaction stoichiometry) assuming that ΔH is constant and that K varies from infinity to ten.

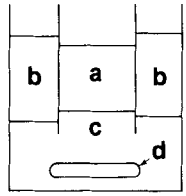

Figure 4. Liquid membrane cell: (a) metal salt-containing source phase, (b) aqueous receiving phase, (c) macrocycle-containing chloroform membrane phase, (d) magnetic stirring bar.

titration procedure (10). This procedure is not limited to any particular solvent.

The liquid membrane used (6,11) is depicted in Fig. 4. Chloroform (3.0 mL) forms the membrane in this system separating two aqueous phases, the source phase (0.80 mL) and the receiving phase (5.0 mL). The experiments were performed at 25°C. The membrane phase containing 0.001 M macrocycle was stirred at 120

rpm by a magnetic stirrer driven by a Hurst synchronous motor. This procedure resulted in the bulk of the liquid membrane being well-mixed. After a period of 24 hours, a 3 mL sample was withdrawn from the receiving phase and the number of moles of cation was determined either by ion chromatography (Dionex Model 10) (Rb^+, Cs^+) or by atomic absorption spectrophotometry (Perkin-Elmer Model 603) (all other cations). Where the amount of cation transported is small, the increase in cation concentration in the receiving phase is linear with time. Three separate cells were used for each salt-macrocycle system to determine the reproducibility of the transport rates. Blank experiments (no macrocycle present) showed that cation leakage across the membrane was always less than 3×10^{-8} mole/24 hours. It is emphasized that the cation transport results are valid only for the particular set of experimental conditions used. Therefore, these results are useful for comparison purposes among themselves, but not with transport data obtained using other conditions, i.e., different stirring rates, different anions, different transport path lengths, etc.

RESULTS AND DISCUSSION

In the following sections we review our published work on selective complexation in CH_3OH of cations by macrocycles, the dependence of J_M on log K in our carrier-mediated liquid membranes, and the development of a cation transport model correlating log K and J_M. We then present and discuss a modification of this model which allows for the simultaneous transport of cations from binary cation mixtures.

Selective Complexation of Cations by Macrocycles

It would be desirable to know $K(CHCl_3)$ values for cation-macrocycle interaction in order to correlate these values with J_M

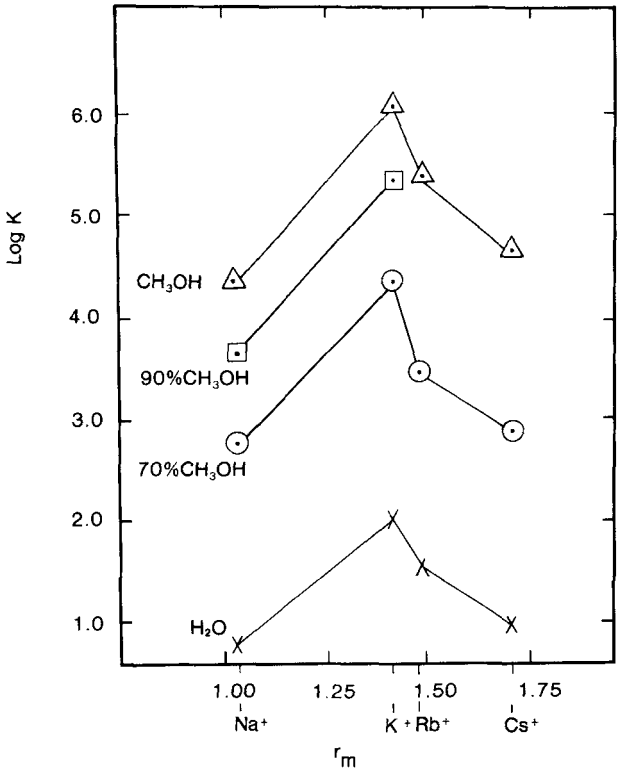

FIGURE 5. Plot of log K vs. cation radius (Å) for reaction M^+ + 18C6 = $M18C6^+$ in water, methanol, and mixtures of the two solvents.

values for our liquid membrane system. Unfortunately, these K values are unknown. However, a large number of $K(CH_3OH)$ values are available for these interactions (5,9,12). The data in Fig. 5 show (a) the selective complexation by 18-crown-6 of K^+ among the other alkali metal ions (9) and (b) the regular increase in log K for reaction (1) for each cation in going from water solvent to methanol (13). The regular variation of log K with solvent composition seen in Figure 5 together with other data for macrocycle-cation interaction in the lower dielectric constant solvents ethanol and n-propanol (13) lead us to make the assumption that

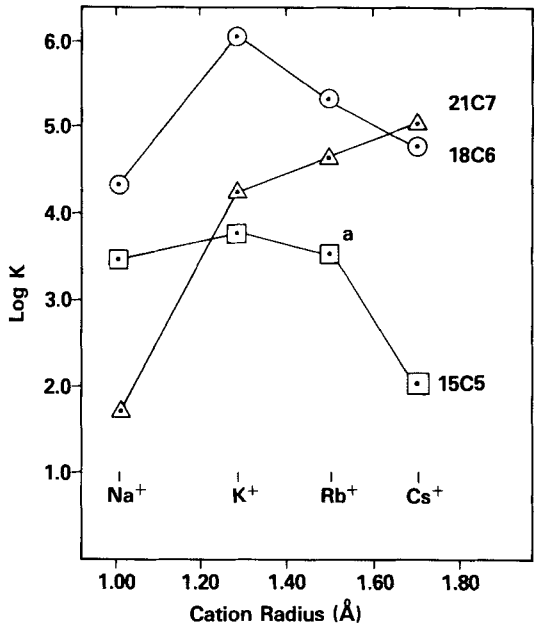

FIGURE 6. Plot of log K for interaction of 15C5, 18C6, and 21C7 with alkali metal cations in methanol at 25°C vs. cation radius (A). (a) Log K value estimated from data valid in water (9).

log K(CH_3OH) values can be used for correlations with J_M, and that the relative order of cation selectivity by macrocycles will be maintained in our chloroform liquid membrane system. The relationship between K for macrocycle-cation formation and dielectric constant has been discussed (13). Comparison of log K(CH_3OH) values for numerous metal-macrocycle systems (9,12) shows that log K, and in some cases, cation selectivity can be altered significantly by varying the macrocycle cavity diameter (Fig. 6), macrocycle substituents (Fig. 7), and ligand donor atom (Fig. 7).

Dependence of Cation Transport Rates on Complex Stability

Schultz and his coworkers in a review (14) on work with facilitated transport in impregnated membranes noted that J_M

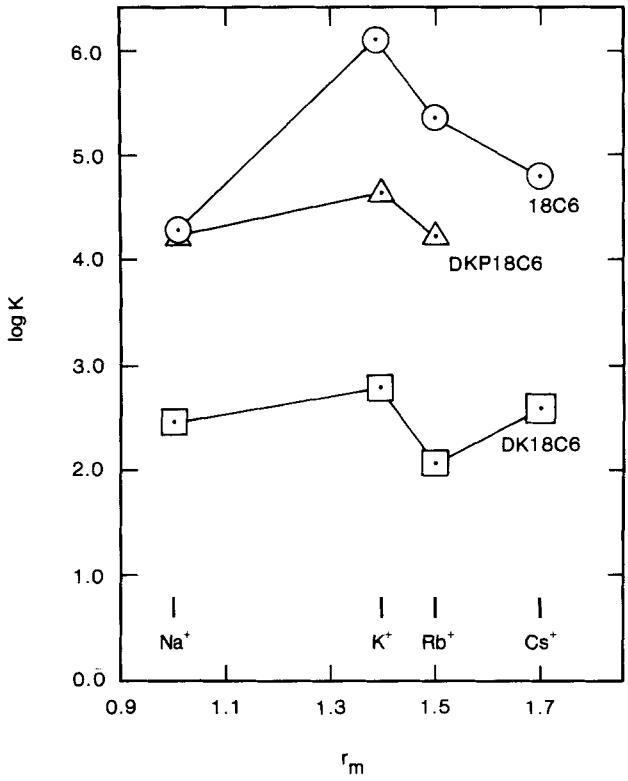

FIGURE 7. Plot of log K vs. cation radius (Å) for 18C6, 2,6-DKP18C6, and 2,6-DK18C6 in methanol at 25°C.

reached a maximum at intermediate log K values. Kirch and Lehn (15), using a chloroform liquid membrane system similar to ours, correlated macrocycle-mediated J_M values with $K(CH_3OH)$ values and pointed out that an optimum value of K exists above or below which the rate of transport decreases. Using a larger variety of macrocyclic ligands, we (7) have confirmed this hypothesis as seen in Fig. 8. Each point in Figure 8 represents a cation-macrocycle system for which both J_M and log $K(CH_3OH)$ are known. For the systems depicted in Fig. 8, maximum transport occurs at approximately log K = 5.5-6 for univalent cations and at a somewhat

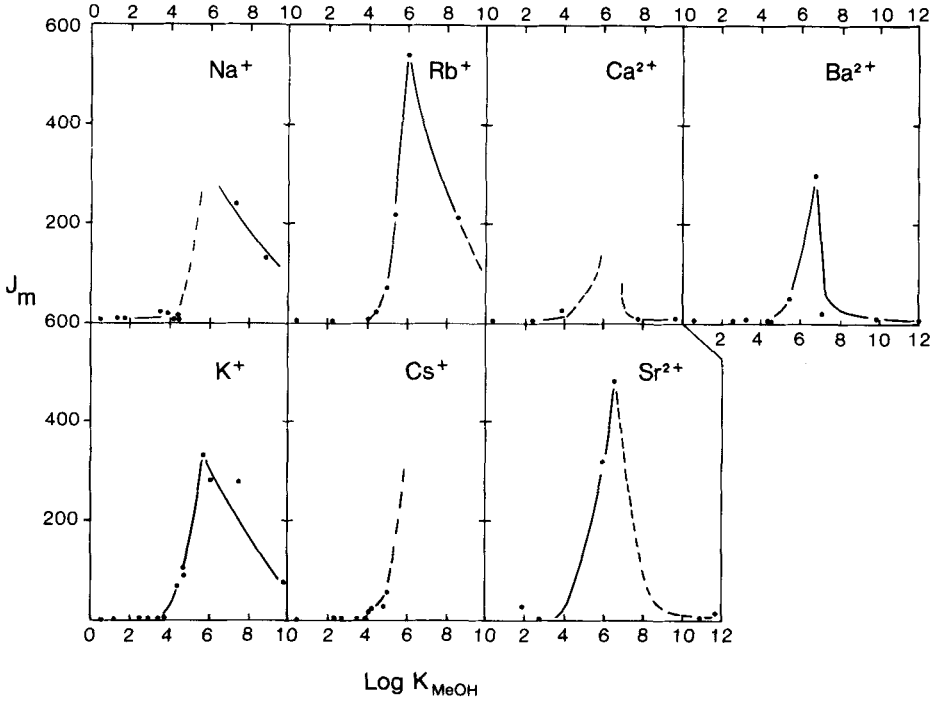

FIGURE 8. Plots of J_M (moles x 10^7/24 hr) vs. log K (methanol, 25°C) using macrocyclic carriers in a chloroform membrane.

higher log K value for bivalent cations. No measurable transport occurs below a log K value of approximately 3.5-4.0. Lack of cation transport at low log K values has been ascribed (7) to lack of appreciable cation-macrocycle interaction. Decreased transport rates at high log K values are attributed to the formation of a stable complex which is little dissociated at the receiving phase boundary.

Cation Transport Model

In liquid membrane systems such as that shown in Figure 4, the relationship between the thermodynamic stability constants for

cation-macrocycle complexation in the membrane and the rates of individual cation transport was predicted by Reusch and Cussler (16) to follow the equation:

$$J_M = \frac{D_c k K L_T M_1^2}{\ell} \qquad (3)$$

where J_M is the flux of cations through the membrane interface, D_c the diffusion coefficient of the complex or the free ligand (the diffusion coefficients of these two species are assumed to be equal), L_T the total ligand (complexed and uncomplexed) concentration in the membrane, M_1 the monovalent cation concentration in the source phase, ℓ the membrane boundary layer thickness and K the stability constant (Eq 2) of the cation-macrocycle complex in the membrane. Equation (3) correctly describes the variation of J_M with log K at low log K values where J_M rises exponentially with log K, but not at high log K values where J_M drops off. A cation transport model has been developed by us using principles similar to those of Reusch and Cussler. Using this model, the change in J_M with log $K(CH_3OH)$ can be predicted over a wide range of log K values including those above the peak in J_M (7). The mechanism of cation transport is similar to that used by Reusch and Cussler and may be expressed in six steps:

(i) $(M_1^+ + A_1^-)_{\text{source phase}} = (MA)_{\text{membrane}}$

(ii) $(MA)_{\text{membrane}} + L_{\text{membrane}} = (MLA)_{\text{membrane}}$

(iii) $(MLA)_{\text{membrane}}$ diffuses across membrane

(iv) $(MLA)_{\text{membrane}} = L_{\text{membrane}} + (MA)_{\text{membrane}}$

(v) $(MA)_{\text{membrane}} = M^+_{\text{receiving phase}} + A^-_{\text{receiving phase}}$

(vi) $(L)_{\text{membrane}}$ diffuses back across membrane.

In the above formulation, the following symbols are used: M^+, cation; A^-, anion; (MA), cation-anion pair; L, macrocyclic ligand;

(MLA), cation complex associated with anion. Step (i) (the inverse of step (v)) is described by a partition coefficient, k, while step (ii) (the inverse of step (iv)) is described by the stability constant, K. In the development of this mechanism, the equilibrium steps (i), (ii), (iv) and (v) are assumed to be rapid with respect to the diffusion steps, (iii) and (vi).

The liquid membrane system used in this theoretical development is given schematically in Figure 9. Vertical lines 2 and 7 represent the interfaces between source and membrane phases and membrane and receiving phases, respectively. In this scheme ℓ_1 represents the boundary layer thickness for mass transfer in the source phase, ℓ_2 is the average distance the ion pair travels in the organic phase before it reaches equilibrium with the ligand, ℓ_3 is the boundary layer thickness for mass transfer of the ligand complex in the organic phase between the source interface and the bulk concentration in the organic phase, ℓ_4 is the boundary layer thickness for the mass transfer of the ligand-ion complex between the bulk organic phase and the receiving phase, ℓ_5 is the average distance the free ion pair travels from the point where it is in equilibrium with the ligand to the receiving phase interface, and ℓ_6 is the receiving phase boundary layer thickness for mass transfer of the metal ion in the aqueous receiving phase. It was assumed that $\ell_1 = \ell_6$, $\ell_2 = \ell_5$, and $\ell_3 = \ell_4$. The distances ℓ_2 and ℓ_5 are a function of the kinetics and concentrations of the species and will vary with ligand but were assumed to be constant for each metal ion. The distances ℓ_1, ℓ_3, ℓ_4, and ℓ_6 are mainly a function of stirring rate, the properties of the fluids, and diffusivities. All of these were nominally constant during the experiments thus these values were held constant for all the theoretical cases. It is assumed that (i) the system is at steady state since the concentrations in the source and receiving phases change little during the time of the run and the length of the run (24 h) is large compared to the transient time which is on the order of 5 minutes, (ii) the diffusivities in the membrane of the free ligand and of the ligand-metal ion complex are equal, and

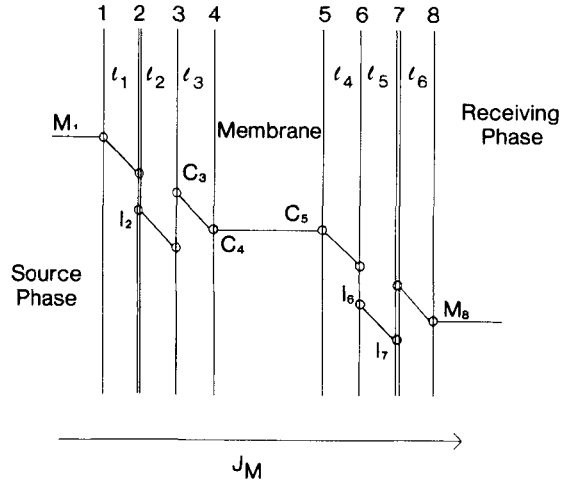

FIGURE 9. Model of membrane interfaces and boundary layers used to derive Eq. 4 (see text).

(iii) the bulk velocity of the water boundary layer normal to the membrane interface is zero. From these considerations the following equation was derived:

$$J_M = \left(\frac{D_c K L_T}{\ell_3 + (a_1/a_2)\ell_4}\right) \left(\frac{(k(M_1 - (J_M\ell_1/D_W))^n - (J_M\ell_2/D_I)}{1 + K(k(M_1-(J_M\ell_1/D_W))^n-(J_M\ell_2/D_I)} - \frac{k(M_8 + (a_1/a_2)(J_M\ell_6/D_W))^n + (a_1/a_2)(J_M\ell_5/D_I)}{1 + K(k(M_8 + (a_1/a_2)(J_M\ell_6/D_W))^n + (a_1/a_2)(J_M\ell_5/D_I)}\right) \quad (4)$$

where n = 2 for monovalent and n = 3 for divalent cations and where a_1 and a_2 represent the areas of the source/membrane and receiving/membrane interfaces, respectively, and D_I and D_W represent the diffusion coefficients of the ion pair MA in the solvent and of the metal ion in the water, respectively.

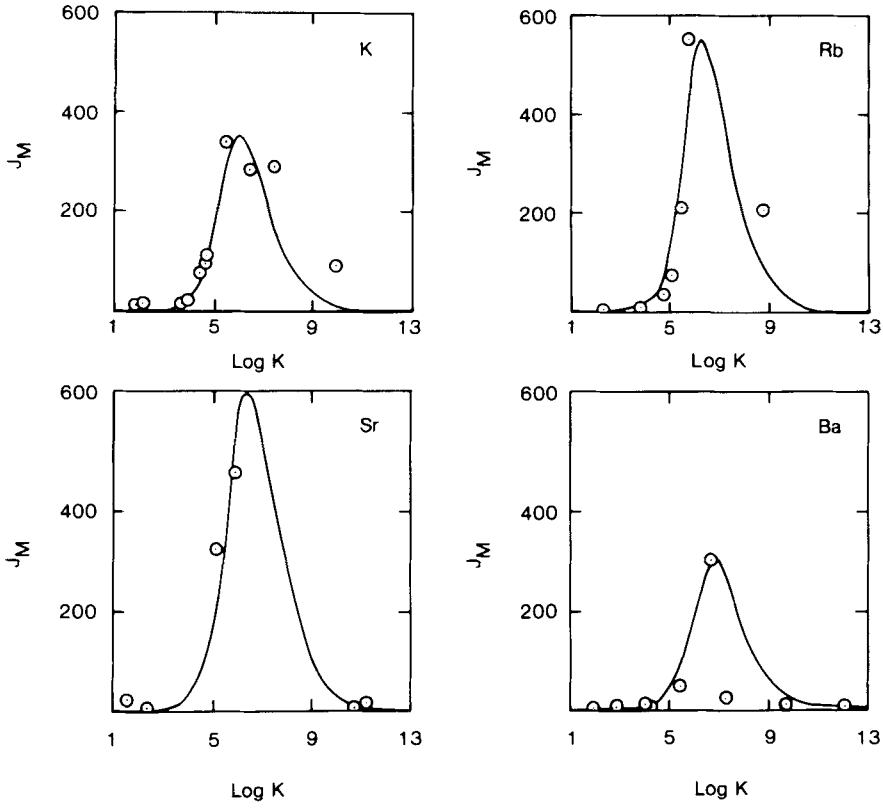

FIGURE 10. Plots of log K (methanol, 25°C) vs. J_M (moles x 10^7/24 hr) including data points (θ) and calculated curves (solid line) from Eq. 4.

Eq. 4 reduces to a form comparable to that of Eq. 3 at small values of k and J_M, and when $M_1 >> M_8$ and $a_1 = a_2$. Therefore, the dependence of J_M on M_1, L_T and anion type correctly described by Eq. 3 are also correctly described by Eq. 4.

Eq. 4 has at least two positive real roots. One set of roots correctly predicts the shape of J_M vs. log $K(CH_3OH)$ curves. In Fig. 10, the calculated J_M vs. log $K(CH_3OH)$ curves are compared to the experimental data for K^+, Rb^+, Sr^{2+}, and Ba^{2+} transport. The values of parameters in Eq. 4 which were used to produce the

TABLE 1

Values of Parameters for Data Fits in Figures 10 and 11.

Parameter	Value (Eq. 4)	Value (Eq. 5)[d]
L_T	1.0 mM	
M_1	1.0 M for K^+, Rb^+ and Sr^{2+}	0.5M for all cations
	0.30 M for Ba^{2+}	
a_1/a_2	0.245	
M_8	1.0 mM	
D_W	1.57×10^{-5} cm^2/sec[a]	
D_c	1.4×10^{-5} cm^2/sec[a]	
D_I	1.8×10^{-5} cm^2/sec[a]	
$\ell_1=\ell_6$	0.013 cm[b]	
$\ell_3=\ell_4$	0.0048 cm[b]	
$\ell_2=\ell_5$	2×10^{-5} cm (K^+)[c]	2×10^{-6} cm (Cs^+)[c]
	5×10^{-6} cm (Rb^+)[c]	5×10^{-6} cm (others)[c]
	3×10^{-6} cm (Sr^{2+})[c]	
	2×10^{-6} cm (Ba^{2+})[c]	
k	3×10^{-6} ℓ/mole (K^+)[c]	2.5×10^{-6} (Cs^+),[c] 21C7
	2×10^{-6} ℓ/mole (Rb^+)[c]	3×10^{-6} (others),[c] 21C7
	2×10^{-6} $(\ell/mole)^2$ (Sr^{2+})[c]	2×10^{-6} (all ions),[c] 18C6
	8×10^{-6} $(\ell/mol)^2$ (Ba^{2+})[c]	

[a]From principles in (17). [b]From principles in (18). [c]Adjusted to give best data fit (13). [d]Only values varied from Eq. 4 are listed.

theoretical curves shown in Fig. 10 are listed in Table 1, as taken from Lamb, et al (13). Adjustment of ℓ_2, ℓ_5, and k was used to fit the theoretical curves to the experimental data.

The diffusion model described by Eq 4. makes it possible to explain the drop in J_M with increasing log K at high log K values without invoking the rate constant for complex dissociation. As log K increases beyond a certain value, the amount of uncomplexed

cation found in the membrane at the receiving phase interface (I_6 in Fig. 9) decreases. Since the rate of diffusion across the membrane-receiving phase interface (and hence the rate of accumulation of cation in the receiving phase) is governed by the differences in concentrations across the boundary layers at that interface, J_M decreases as I_6 decreases. In Fig. 10 the solid line is derived from Eq. 4 and it is seen that excellent agreement is found between it and the experimental points. Thus, we conclude that carrier-mediated transport in our single cation system is accounted for by this diffusion model.

Cation Transport from Binary Cation Mixtures

The selectivity of macrocycle-containing membranes may be exploited by selectively transporting cations from cation mixtures. We have accomplished selective transport of Pb^{2+} (19), Sr^{2+} (20), and Cs^+ from binary cation mixtures using a large variety of macrocycle carriers. The selectivity of membranes of this type is excellent. For instance, DCy18C6 is very selective in transporting Pb^{2+} over Li^+, Na^+, K^+, and Sr^{2+} (Table 2) and several other cations as well (19). While selectivity for Cs^+ is not as dramatic as that for Pb^{2+}, Cs^+ transport from binary Cs^+-M^+ systems can be used to illustrate some of the features associated with selective membrane transport.

In Table 3 are presented relative transport rates for Cs^+ and M^+ from binary cation mixtures using chloroform membranes containing either 18C6 or 21C7. In these cases log $K(CH_3OH)$ values are available (9). The log K value in the case of Cs^+ falls intermediate among those of the remaining cations for 18C6, but is larger than that of any of the other cations in the case of 21C7.

We have modified the model described by Eq. 4 to predict the macrocycle-mediated transport rate of Cs^+ from binary mixtures of that cation with other M^+ cations. The model, which is general, assumes the transport of two cations simultaneously and is based

TABLE 2

Selectivity for Pb^{2+} in Binary Cation Mixtures using a Chloroform Membrane Containing DCy18C6 (19).

Ratio of Moles Transported x 10^7/24hr							
Pb^{2+}/Li^+		Pb^{2+}/Na^+		Pb^{2+}/K^+		Pb^{2+}/Sr^{2+}	
Together	Separate	Together	Separate	Together	Separate	Together	Separate
300/0	320/1	240/1	320/23	270/2	320/340	330/6	320/450

TABLE 3

Relative Transport Rates (x 10^7 moles/24 hr) for Several Cs^+/M^+ Mixtures Using Chloroform Membranes Containing either 18C6 or 21C7 and Log $K(CH_3OH)$ Values for Several M^+-L Systems Valid for Reaction (1) at 25°C.

Ligand	J_M Values			
	Cs^+/Li^+	Cs^+/Na^+	Cs^+/K^+	Cs^+/Rb^+
18C6	$\frac{52}{0.07}$	$\frac{33}{32}$	$\frac{11}{240}$	$\frac{28}{250}$
21C7	$\frac{65}{0.09}$	$\frac{67}{1.9}$	$\frac{72}{60}$	$\frac{81}{70}$

Log $K(CH_3OH)$ Values

	Li^+	Na^+	K^+	Rb^+	Cs^+
18C6	<0.5	4.36	6.06	5.32	4.79
21C7	<0.1	1.73	4.22	4.86	5.01

on the same assumptions and development as reported earlier for the transport of a single species (Eq. 4 and reference (7)). The only difference between the two models is that, in the present one, consideration must be given to two cation-macrocycle stability constants, two ion pair interactions in the organic phase, two partition coefficients, and two distances travelled by the ion pair in the organic phase before equilibrium is reached, one for each metal ion.

Including the effects of two metal ion species with the assumptions used in developing Eq. 4 gives Eq. 5 for the flux of the first cation species J_{Mf}. The equation for the flux of the second cation species J_{Ms}, is the same except that subscript s is exchanged for subscript f. The above equations were solved simultaneously using a Newton Raphson iteration on a VAX/11-780 computer.

The lines in Figure 11a and 11b show the computer-generated predicted transport of Cs^+ (dashed) against any second univalent cation, M^+, (solid) having a log K value given on the abscissa using 18C6 and 21C7, respectively, as carriers. The predicted transport of M^+ corresponding to log K values valid for M^+ can be read from the solid lines in (a) and (b). The experimental J_{Mi} (i may be either f or s) and log $K(CH_3OH)$ values for Na^+, K^+, and Rb^+ (Table 3) are compared (vertically) with J_M values for Cs^+ using dots enclosed by circles. The agreement with the model is good. It should be noted that only log K and J_{Mi} values have been varied in this correlation. However, different partition coefficients were used for 18C6 and 21C7 to reflect their different solubilities in the two phases. It is expected that better agreement between the model and measured J_{Mi} values would be obtained if measured ligand and metal complex partition coefficient values, and log K values for ion pair formation in the organic phase were included. Unfortunately, these values are unknown.

The bulk chloroform liquid membranes used in this work do not have potential for industrial application. In addition, the aqueous solubilities of the macrocycles used here are much too

$$J_{Mf} = \left(\frac{D_{cf} K_f L_T}{\ell_3 + (a_1/a_2)\ell_4} \right) \left(\frac{k_f [M_{1f} - (J_{Mf}\ell_1/D_{Wf})]^{nf} - J_{Mf}\ell_{2f}/D_{If}}{1 + K_f [k_f (M_{1f} - J_{Mf}\ell_1/D_{Wf})^{nf} - J_{Mf}\ell_{2f}/D_{If}] + K_s [k_s (M_{1s} - J_{Ms}\ell_1/D_{Ws})^{ns} - J_{Ms}\ell_{2s}/D_{Is}]} - \right.$$

$$\left. \frac{k_f [M_{8f} + (a_1/a_2)(J_{Mf}\ell_6/D_{Wf})]^{nf} + (a_1/a_2)(J_{Mf}\ell_{5f}/D_{If})}{1 + K_f \{k_f [M_{8f} + (a_1/a_2)(J_{Mf}\ell_6/D_{Wf})]^{nf} + (a_1/a_2)(J_{Mf}\ell_{5f}/D_{If})\} + K_s \{k_s [M_{8s} + (a_1/a_2)(J_{Ms}\ell_6/D_{Ws})]^{ns} + (a_1/a_2)(J_{Ms}\ell_5/D_{Is})\}} \right) \quad (5)$$

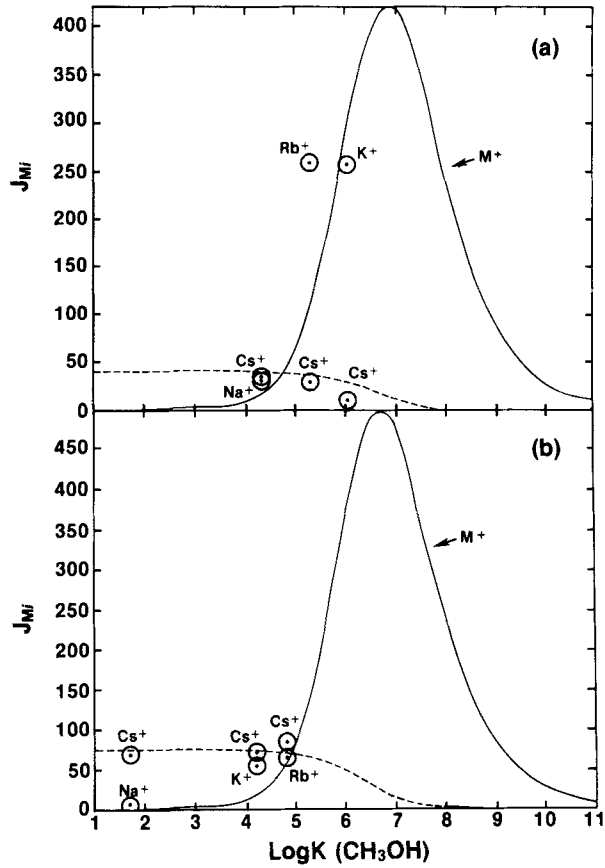

FIGURE 11. Plots of experimental (Table 3) and calculated (from Eq. 5) log K and J_{Mi} values for 18C6 (a) and 21C7 (b).

large for them to be of interest in practical applications. However, water-insoluble derivatives of DCy18C6 in which an H on each cyclohexo group is replaced by a $C_{10}H_{21}$ group have been found to transport alkali and alkaline earth cations as well as DCy18C6 in our system (6). Other liquid membranes have been designed so as to minimize membrane thickness and maximize membrane surface area. Examples of such membranes include the liquid surfactant

membranes of Li and his coworkers (21) and liquid membranes of the diaphragm type, with the membrane supported on a porous polymer network (22). The study of simple, well-defined membranes of the type presented here is being used to assist in incorporating macrocycles into these more efficient membrane systems.

ACKNOWLEDGMENT

The research reported here was sponsored by the U.S. Department of Energy under Contract Number DE-AC02-78ER05016.

REFERENCES

1. C.J. Pedersen, J. Am. Chem. Soc., 89, 7017 (1967).

2. J.S. Bradshaw, in Synthetic Multidentate Macrocyclic Compounds (R.M. Izatt and J.J. Christensen, eds.), Academic Press, New York, 1978.

3. C.J. Pedersen, in Synthetic Multidentate Macrocyclic Compounds (R.M. Izatt and J.J. Christensen, eds.), Academic Press, New York, 1978.

4. N.K. Dalley, in Synthetic Multidentate Macrocyclic Compounds (R.M. Izatt and J.J. Christensen, eds.), Academic Press, New York, 1978.

5. J.D. Lamb, R.M. Izatt, J.J. Christensen, and D.J. Eatough, in Coordination Chemistry of Macrocyclic Compounds (G.A. Melson, ed.), Plenum Press, New York, 1979.

6. J.D. Lamb, R.M. Izatt, D.G. Garrick, J.S. Bradshaw, and J.J. Christensen, J. Membr. Sci., in press.

7. J.D. Lamb, J.J. Christensen, J.L. Oscarson, B.L. Nielsen, B.W. Asay, and R.M. Izatt, J. Am. Chem. Soc., 102, 6820 (1980).

8. J.D. Lamb, J.E. King, J.J. Christensen, and R.M. Izatt, Anal. Chem., in press.

9. J.D. Lamb, R.M. Izatt, C.S. Swain, and J.J. Christensen, J. Am. Chem. Soc., 102, 475 (1980).

10. D.J. Eatough, R.M. Izatt, and J.J. Christensen in Thermometric Methods in Clinical Analysis (N. Jespersen, ed.), Elsevier, New York, in press.

11. J.D. Lamb, J.J. Christensen, S.R. Izatt, K. Bedke, M.S. Astin, and R.M. Izatt, J. Am. Chem. Soc., 102, 3399 (1980).

12. J.D. Lamb, R.M. Izatt, C.S. Swain, J.S. Bradshaw, and J.J. Christensen, J. Am. Chem. Soc., 102, 479 (1980).

13. J.D. Lamb, R.M. Izatt, and J.J. Christensen, in Progress in Macrocyclic Chemistry, Volume 2 (R.M. Izatt and J.J. Christensen, eds.), Wiley-Interscience, New York, 1981.

14. J.S. Schultz, J.D. Goddard, and S.R. Suchdeo, A.I.Ch.E. J., 20, 417 (1974).

15. M. Kirch and J.M. Lehn, Angew. Chem. Intern. Ed. Engl., 14, 555 (1975).

16. C.F. Reusch and E.L. Cussler, A.I.Ch.E. J., 19, 736 (1973).

17. R.C. Reid, J.M. Prausnitz, and T.K. Sherwood, The Properties of Gases and Liquids, 3rd ed., McGraw-Hill, New York, 1977, pp. 566-582.

18. R.B. Bird, W.E. Stewart, and E.N. Lightfoot, Transport Phenomena, Wiley, New York, 1960.

19. J.D. Lamb, R.M. Izatt, P.A. Robertson, and J.J. Christensen, J. Am. Chem. Soc., 102, 2452 (1980).

20. Unpublished results, this laboratory.

21. R.P. Cahn and N.N. Li, Sep. Sci., 9, 505 (1974); T.H. Maugh II, Science, 193, 134 (1976).

22. W.C. Babcock, R.W. Baker, E.D. LaChapelle, and K.L. Smith, J. Membr. Sci., 7, 71 (1980).